Elucidating Si−Si Dimmer Vibration from the Size-Dependent Raman Shift of Nanosolid Si

L. K. Pan, Chang Q. Sun,* and C. M. Li

School of Electrical and Electronic Engineering, Nanyang Technological University, Singapore 639798

Received: December 16, 2003

It has been surprising that with the solid size reduction, the transverse optical (TO) Raman mode shifts to lower frequency and new low-frequency Raman (LFR) acoustic modes are generated and shift to higher frequency upon nanosolid Si formation. Understanding the mechanism behind the TO red shift and the LFR creation and blue shift has long been a challenge. On the basis of the BOLS correlation [Sun et al. *J. Phys. Chem. B* **2002**, *106*, 10701], here we show that the TO red shift arises from the cohesive bond weakening of the lower coordinated atoms near the surface region of the nanograin, and the LFR arises from intergrain interaction. Strikingly, simulating the TO peak shift confirms the assumption, originated by Shi and Jiang, that the magnitude of surface atomic vibration is always higher than the bulk value and remains constant at particle size greater than 1 nm. Practice also provides a way for elucidating information of an isolated Si−Si dimer vibration.

Vibration of atoms at a Si surface is of increasing interest because the behavior of phonons has direct influence on the electrical and optical properties in semiconductor nanosolids, such as electron−phonon coupling, photoabsorption, and photoemission.[1] The frequency of transverse optical (TO) phonon undergoes a red shift[2] whereas the low-frequency Raman (LFR) modes are generated with blue shift[3] upon the radius R of Si nanosolid being decreased. The TO red shift has been explained in terms of surface stress[4,5] and phonon quantum confinement,[6,7] as well as surface chemical passivation.[8] However, the effect of stress is usually ignorable for hydrogenated silicon,[9−11] in which hydrogen atoms terminate the surface bond network, which reduce bonding strains and hence the residual stress. Phonon confinement model[6] attributes the red shift of the asymmetric Raman line to relaxation of the q-vector selection rule for the excitation of the Raman active optical phonons due to their localization. When the size is decreased, the momentum conservation will be relaxed and the Raman active modes will not be limited to be at the center of the Brillouin zone.[4] A Gaussian-type phonon confinement model[7] that has been used to fit the experimental data indicates that strong phonon damping exists in the nanosolid. Calculations[12] using the correlation functions of the local dielectric constant disregarding the role of phonon damping in the nanosolid refer the TO Raman red shift to the relaxation of the momentum conservation rules due to the finite crystalline size and the diameter distribution of nanosolid in the films. In contrast to the TO red shift, LFR features are created upon nanosolid formation. The LFR peaks are squeezed to the blue side.[3,13] The size-dependent blue shift is also attributed to acoustic phonons confined in the nanosolid silicon. The size dependent Raman shift is expressed as[2,13]

$$\Delta\omega(R) = \omega(R) - \omega(\infty) = A(a/R)^{\kappa} \qquad (1)$$

where A and κ are adjustable parameters used to fit the measured data. For the TO red shift, $A < 0$ and $\omega(\infty) = 520$ cm^{-1} (corresponding to wavelength of 2×10^4 nm). The κ varies from 1.08 to 1.44 and 2.0.[14] The a is the lattice parameter that contracts with the solid dimension.[15] For LFR blue shift, $A > 0$, $\kappa = 1$, and $\omega(\infty) = 0$. Therefore, the LFR results from nanosolid formation. The currently available models for the TO red shift are based on assumptions that the materials are homogeneous and isotropic, which is valid only in the long-wavelength limit. When the size of the nanosolid is in the range of a few nanometers, the continuum dielectric models are intrinsically limited. Therefore, the existing models could hardly reproduce satisfactorily the Raman frequency shifts near the lower end of the size limit though they contribute to the understanding from various perspective. Therefore, deeper insight into the physical origin of the blue and red shift is desirable.

Raman scattering is known to arise from the radiating dipole moment induced in a system by the electric field of incident electromagnetic radiation. The laws of momentum and energy conservation govern the interaction between a phonon and a photon. The total energy E due to the lattice vibration consists of the component of short-range interactions E_S and the component of long-range Coulomb interaction E_C,[13]

$$E = E_S + E_C \qquad (2)$$

The short-range interaction corresponds to the TO mode, which describes the covalent bonding and thus is correlated to bond energy E_b, bond length d, and the coordination number (CN, or z). The long-range part corresponds to the LFR mode and represents the weak interaction between nanosolids.

Figure 1 shows the least-squares fitting of the size dependent LFR frequency for the nanosolid silicon. The LFR frequency depends linearly on the inverse R. The zero intercept at the vertical axis indicates that when R increases toward infinity, the LFR peaks disappear, which implies that not only the blue shift in the LFR peaks but also the origin for the LFR peaks are purely intergrain vibrations that produce acoustic phonons. The slope values are 97.77, 45.57, and 33.78 for the A_1, T_2, and E modes, corresponding to the stretching (*LA*) and bending (*TA*), respectively.

For the Raman TO mode, the energy due to short-range interaction of a single pairwise bond can be expressed in a

* E-mail: ecqsun@ntu.edu.sg. Fax: 65 6792 0415. http://www.ntu-.edu.sg/home/ecqsun/.

10.1021/jp037891s CCC: $27.50
Published on Web 02/19/2004

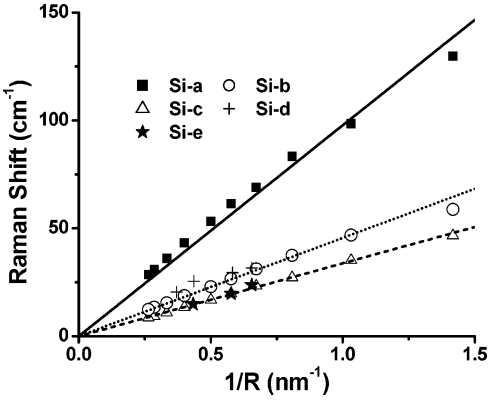

Figure 1. Generation and blue shift of the LFR spectra where the solid, dotted, and dashed lines are the corresponding results of the least-squares fitting. The Si-a (A_1 mode), Si-b (T_2 mode), and Si-c (E mode) are calculated from the lattice-dynamic matrix by using a microscopic valence force field model.[13] Si-d and Si-e are the experimental results.[3]

Taylor's series

$$E_S = \sum_{n=0}\left(\frac{d^n u(r)}{n!dr^n}\right)_{r=d}(r-d)^n = u(d) + 0 + \frac{d^2u(r)}{2!dr^2}\Big|_d (r-d)^2 + ... \quad (3)$$

When the atom is in the equilibrium position, the bond energy is $u(d) = E_b$. The third term is the vibration energy of a single bond due to the short-range interaction, in which the force constant $k = d^2u(r)/dr^2|_d \propto E_b/d^2$ and the vibration amplitude $x = r - d$. For a single bond, the k is strengthened but for a single lower coordinated atom, the resultant k could be lower. Because the short-range interaction on each atom results from its neighboring coordinating atoms, the atomic vibrating dislocation is the contribution from all the surrounding coordinates, z. Considering the vibration amplitude $x \ll d$, it is reasonable to take the mean contribution from each coordinate as a first-order approximation, i.e., $k_1 = k_2 = ... = k_z = \mu_{Si}(c\omega)^2$, and $x_1 = x_2 = ... = x_z = (r - d)/z$. Therefore, the energy due to short-range interaction of a certain atom with z coordinates follows:

$$E_S = \sum_z\left[-E_b + \frac{1}{2}\mu_{Si}c^2\omega^2\left(\frac{r-d}{z}\right)^2 + ...\right] = -zE_b + \frac{1}{2z}\mu_{Si}c^2\omega^2(r-d)^2 + ... \quad (4)$$

where $\mu_{Si} = m_{Si}/2 = 2.34 \times 10^{-26}$ kg is the reduced mass of a Si−Si dimer and c is the speed of light. Equilibrating (4) to (3) times z, we have the phonon frequency (wavenumber, ω) as follows:

$$\omega = \frac{1}{c}\left(\frac{z}{\mu_{Si}}\right)^{1/2}\left[\frac{zd^2u(r)}{dr^2}\Big|_d\right]^{1/2} \propto \frac{z(E_b)^{1/2}}{d} \quad (5)$$

A recent bond-order-length-strength (BOLS) correlation mechanism[16−18] indicates that the CN imperfection causes the remaining bonds of the lower-coordinated atoms to contract spontaneously ($d_i = c_i d$) associated with bond strength enhancement ($E_i = c_i^{-m}E_b$). Such an event and its consequence modify not only the atomic cohesive energy (atomic CN multiplies the single bond energy) but also the binding energy density in the relaxed region. The former contributes to the Gibbs free energy that dictates all the thermodynamic behavior of the considered solid such as critical temperature for phase transition, liquidization, and evaporation;[18] the latter, to the Hamiltonian that dictates the entire energy band structures such as the band gap,[17] core-level shift,[16,19] and the mechanical strength[20] of the system. A physically detectable quantity for a nanosolid can be expressed as $Q(R)$, and as $Q(\infty) = Nq_0$ for a bulk solid. The relation between $Q(R)$ and $Q(\infty)$ and the relative change of Q can be expressed in a shell structure:

$$\begin{cases} Q(R) = Nq_0 + N_S(q - q_0) \\ \dfrac{Q(R) - Q(\infty)}{Q(\infty)} = \displaystyle\sum_{i\le 3}\gamma_i\left[\frac{q_i}{q_0} - 1\right] \end{cases} \quad (6)$$

where q_0 and q_S correspond to the Q value per atomic volume inside the bulk and in the surface region, respectively, $N_S = \Sigma N_i$ is the number of atoms in the surface atomic shells. Combining eqs 5 and 6 give the size-dependent TO red shift:

$$\frac{\omega(R) - \omega(\infty)}{\omega(\infty) - \omega(1)} = \sum_{i\le 3}\gamma_i\left[\frac{\omega_i}{\omega_b} - 1\right] = \sum_{i\le 3}\gamma_i\left[\frac{z_i}{z_b}c_i^{-(m/2)+1} - 1\right] = \delta_p < 0 \quad (7)$$

where[15]

$$\begin{cases} \gamma_i = \dfrac{N_i}{N} = \dfrac{V_i}{V} \approx \dfrac{\tau c_i}{K} \\ c_i = 2/\{1 + \exp[(12 - z_i)/(8z_i)]\} \\ z_1 = 4(1 - 0.75/K) \end{cases} \quad (8)$$

$m = 4.88$, $z_2 = 6$, and $z_3 = 12$ for a silicon spherical dot.[16] $\omega(1)$ is the vibrational frequency of an isolated Si−Si dimer bond, which is the reference point for the TO red shift upon nanosolid and bulk formation ($Q(\infty) = \omega(\infty) - \omega(1)$ is the bulk shift). $d = 0.2632$ nm is the diameter of a Si atom in bulk. γ_i is the portion of atoms in the ith atomic layer compared to the total number of atoms of the entire solid of different dimensionality ($\tau = 1-3$ correspond to a thin plate, a rod, and a spherical dot, respectively). The index i is counted up to three from the outmost atomic layer to the center of the solid as no atomic CN imperfection is justified at $i > 3$. $K = R/d$ is the number of atoms lined along the radius of the nanosolid. Therefore, we can calculate the relative frequency change without needing any assumptions. Incorporating the BOLS prediction with the linearization of measurement, we have the following relations

$$\Delta\omega(R) = \begin{cases} \dfrac{-5.315}{R} & \text{(Measurement)} \\ \delta_p(\omega(\infty) - \omega(1)) & \text{(Theory)} \end{cases} \quad (9)$$

Hence, the frequency shift from the dimer bond vibration to the bulk value, $\omega(\infty) - \omega(1) \equiv -5.315/(\delta_p R)$, is a constant as $\delta_p \propto R^{-1}$. Excitingly, this allows us to determine the vibrational frequency of a Si−Si dimer bond $\omega(1) = 502.3$ cm^{-1} and the bulk shift of 17.7 cm^{-1}, which is beyond the scope of currently available approaches. Figure 2 shows the match between the BOLS predictions with the theoretically calculated and the experimentally measured TO red shift of nanosolid silicon.

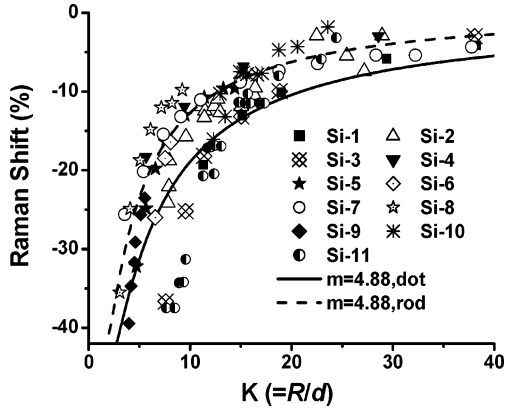

Figure 2. Comparison of the predictions with observations on the size-dependent TO shift of the nanosolid silicon. Theoretical results: Si-1 calculated using correlation length model;[23] Si-3 (dot) and Si-4 (rod) calculated using the bulk dispersion relation of phonons;[24] Si-5 calculated from the lattice-dynamic matrix;[13] Si-7 calculated using phonon confinement model[25] and Si-8 (rod), Si-9 (dot), calculated using bond polarizability model.[2] Measurements: Si-2;[26] Si-6;[27] Si-10 and Si-11.[4] *d* is the bond length of bulk silicon. *K* is the number of atoms arranged along the radius of spherical dot or a rod.

According to Einstein's relation: $z\mu_{Si}\{(c\omega)^2(x/z)^2/2 = k_BT$ (k_B is the Boltzmann constant and T is the temperature), thevibrational amplitude of an atom is $x \propto z^{1/2}\omega^{-1}$. The reduced magnitude and frequency of an atom in the surface at room temperature are

$$\frac{x_1}{x_b} = (z_1/z_b)^{1/2}\omega_b/\omega_1 = (z_b/z_1)^{1/2}c_1^{(m/2)+1} = \begin{Bmatrix} \sqrt{3} \times 0.88^{3.44} = 1.09 & (\text{Si}, m = 4.88) \\ \sqrt{3} \times 0.88^{1.5} = 1.43 & (\text{metal}, m = 1) \end{Bmatrix} \quad (10)$$

As the z_1 change slightly with the curvature of the surface, see eq 8, the vibrational amplitude of an atom at the surface stays almost constant at $K > 3$. This confirms for the first time the assumption originated by Shi[21] and Jiang et al.[22] that the vibrational amplitude of a surface atom is higher than the bulk value and keeps constant at all particle sizes. It can also be estimated that the frequency of a Si surface atom (with $z = 4$) is around 511 cm^{-1}, which is between that of the dimmer (502.3 cm^{-1}) and the bulk (520.0 cm^{-1}).

In summary, the BOLS correlation has enabled us to correlate the size-created and the size-induced blue shift in the LFR phonon frequency to the intergrain interaction and the red shift in the TO phonon frequency to the atomic CN imperfection reduced atomic cohesive energy. Decoding the Raman red shift leads to quantitative information about the vibration frequency of a Si−Si dimer bond (502.3 cm^{-1}) at room temperature and the confirmation of surface atomic dislocation.

References and Notes

(1) Takagahara, T. *Phys. Rev. Lett.* **1993**, *71*, 3577.
(2) Zi, J.; Büscher, H.; Falter, C.; Ludwig, W.; Zhang, K. M.; Xie, X. D. *Appl. Phys. Lett.* **1996**, *69*, 200.
(3) Fujii, M.; Kanzawa, Y.; Hayashi, S.; Yamamoto, K. *Phys. Rev. B* **1996**, *54*, R8373.
(4) Iqbal Z.; Vepek, S. *J. Phys. C* **1982**, *15*, 377.
(5) Anastassakis, E.; Liarokapis, E. *J. Appl. Phys.* **1987**, *62*, 3346.
(6) Richter, H.; Wang, Z. P.; Ley, L. *Solid State Commun.* **1981**, *39*, 625.
(7) Campbell, I. H.; Fauchet, P. M. *Solid State Commun.* **1986**, *58*, 739.
(8) Sun, C. Q. *Prog. Mater. Sci.* **2003**, *48(6)*, 521.
(9) Papadimitriou, D.; Bitsakis, J.; López-Villegas, J. M.; Samitier, J.; Morante, J. R. *Thin Solid Films* **1999**, *349*, 293.
(10) Wang, X.; Huang, D. M.; Ye, L.; Yang, M.; Hao, P. H.; Fu, H. X.; Hou, X. Y.; Xie, X. D. *Phys. Rev. Lett.* **1993**, *71*, 1265.
(11) Andjar, J. L.; Bertran, E.; Canillas, A.; Roch, C.; Morenza, J. L. *J. Vac. Sci. Technol. A* **1991**, *9*, 2216.
(12) Ohtani, N.; Kawamura, K. *Solid State Commun.* **1990**, *75*, 711.
(13) Cheng, W.; Ren, S.-F. *Phys. Rev. B* **2002**, *65*, 205305.
(14) Hwang, Y.-N.; Shin, S.; Park, H. L.; Park, S.-H.; Kim, U.; Jeong, H. S.; Shin, E.-J.; Kim, D. *Phys. Rev. B* **1996**, *54*, 15120.
(15) Sun, C. Q.; Li, S.; Tay, B. K. *Appl. Phys. Lett.* **2003**, *82*, 3568.
(16) Sun, C. Q.; Pan, L. K.; Fu, Y. Q.; Tay, B. K.; Li, S. *J. Phys. Chem. B* **2003**, *107*, 5113.
(17) Pan, L. K.; Sun, C. Q.; Tay, B. K.; Chen, T. P.; Li, S. *J. Phys. Chem. B* **2002**, *106*, 11725.
(18) Sun, C. Q.; Wang, Y.; Tay, B. K.; Li, S.; Huang, H.; Zhang, Y. *J. Phys. Chem. B* **2002**, *106*, 10701.
(19) Sun, C. Q. Surface and Nanosolid Core-level Shift: Impact of Atomic Coordination Number Imperfection. *Phys. Rev. B* **2004**, *69*, 045105.
(20) Sun, C. Q.; Bai, H. L.; Tay, B. K.; Li, S.; Jiang, E. Y. *J. Phys. Chem. B* **2003**, *107*, 7544.
(21) Shi, F. G. *J. Mater. Res.* **1994**, *9*, 1307.
(22) Jiang, Q.; Zhang, Z.; Li, J. C. *Chem. Phys. Lett.* **2000**, *322*, 549.
(23) Viera, G.; Huet, S.; Boufendi, L. *J. Appl. Phys.* **2001**, *90*, 4175.
(24) Fauchet, P. M.; Campell, I. H. *Crit. Rev. Solid State Mater. Sci.* **1988**, *14*, S79.
(25) Sood, A. K.; Jayaram, K.; Victor D.; Muthu, S. *J. Appl. Phys.* **1992**, *72*, 4963.
(26) Ossadnik, C.; Vepek, S.; Gregora, I. *Thin Solid Films* **1999**, *337*, 148.
(27) Cheng, G.-X.; Xia, H.; Chen, K.-J.; Zhang, W.; Zhang, X.-K. *Phys. Status Solidi A* **1990**, *118*, K51.